ESCUELA DE CONSTRUCCIÓN CIVIL
FACULTAD DE INGENIERÍA

Revista de la Construcción
Journal of Construction

Research Article

Experimental investigations the effects of dusty, humidity and temperature conditions on chemical anchors

Özlem Çalışkan [1], Murat Aras [2, *], Yılmaz Ağdağ [3]

[1] Department of Civil Engineering, Bilecik Seyh Edebali University, Bilecik (Turkey); ozlem.caliskan@bilecik.edu.tr
[2] Department of Civil Engineering, Bilecik Seyh Edebali University, Bilecik (Turkey); murat.aras@bilecik.edu.tr
[3] Agdag Construction Limited Company, Bilecik (Turkey); y.agdag@gmail.com
*Correspondence: murat.aras@bilecik.edu.tr

Received: 18.05.2022; **Accepted:** 15.09.2023; **Published:** 29.12.2023

Citation: Çalışkan Ö., Aras, M. and Ağdağ, Y. (2023). Experimental investigations the effects of dusty, humidity and temperature conditions on chemical anchors. Revista de la Construcción. Journal of Construction, 22(3), 613-631. https://doi.org/10.7764/RDLC.22.3.613.

Abstract: Chemical anchor applications are frequently used to add new structural elements to existing structures. Chemical anchors can be applied quickly and easily, if anchors apply according to a detailed installation and cleaning procedure depending on environmental conditions and workmanship. In this work, the relationship between the axial tensile capacity of chemical anchors and the effect of dust, humidity, and temperature were examined as adverse conditions. The effect of using different conditions, anchorage diameters and embedment depth on the tensile strength of the anchors was evaluated. In the experimental study, anchors diameter 12, 16 and 20 mm were selected to be used as anchors. The depth of embedding was determined to be 5, 10, 15 and 20 times the diameter of used anchors. The initial stiffness, displacement ductility ratio, energy absorption capacity, failure modes, and safety levels according to ACI 318 were obtained by using the load-displacement curves. According to the parameters considered in the experimental program, the most unfavorable situation was obtained in anchors embedded in a wet environment. In addition, it was observed that the diameter of the drilled holes causes a decrease in the axial tensile capacity by increasing the exposure time of the anchors to water and temperature.

Keywords: chemical anchor, pull-out test, dust, humidity and temperature effects, ACI 318.

1. Introduction

Anchors in concrete are generally divided into two main groups in terms of placement time and type: anchors in fresh and hardened concrete. Anchors planted in hardened concrete with an adhesive are called chemical anchors. Chemical anchors are widely used for the connection of new elements to be added to reinforced concrete structures because they are fast and easy to apply. When a new element is added to the structural system, the interlocking of the old and new elements depends on the interlocking between the reinforcement, chemical adhesive and concrete (Cook, 1993). The anchors are exposed to tensile, shear and, bearing loads generated by reinforcement systems such as shear walls or reinforced concrete shells. With these reinforcements, it is possible to ensure that existing and new concrete elements resist seismic forces together without compromising the safety of the structure. In addition, anchors are commonly used for the erection of precast elements in industrial structures and power plant structural element assemblies that are exposed to high temperatures. Therefore, great care should be taken in the application of chemical anchors. The performance of the chemical anchor depends on the planting depth, the distance between the edges and anchors, the properties of the adhesive to be used, the cleanliness, humidity and

temperature of the place where the anchor will be planted. It is important to choose the appropriate material for the place to be used in order to obtain the desired performance. It has been observed that chemical adhesives used for the same purpose can give different results in terms of tensile strength (Bajer and Barnat, 2012; Çalışkan and Aras, 2017). Chemical adhesives are known as epoxy or resin. In recent years, the use of chemical anchors has increased in the repair and strengthening works of buildings, and in adding forgotten or additional reinforcement. Thus, the importance of chemical adhesives has gradually increased. Chemical adhesives can be polyester, vinylester, epoxy based or epoxy acrylate based (Cook, 1993, Çalışkan and Aras 2017). Apart from chemical adhesives, anchor rods can also be planted with mortar called grout (Porcarelli, et al. 2021).

Chemical anchors can be subjected to tensile (McVay et al. 1996; Obata et al. 1998; Zamora et al. 2003; Shirvani et al. 2004; Kim et al. 2013), shear (Caliskan et al. 2013, Bokor et al. 2020) and tension-shear (Epackachi et al. 2015, Takase, 2019) loading. In practice, anchors are planted more than once and work in groups (Stehle and Sharma 2021, Vita et al. 2022). In chemical anchors, interlocking occurs through the friction force between the chemical and the anchor reinforcement and concrete. In order to ensure full interlocking, the appropriate material must be selected. The parameters affecting the axial tensile behavior of chemical anchors are mechanical and physical properties of the chemical adhesive used, area of use, type of use, ambient conditions, humidity, cleanliness of the holes, quality of workmanship, distance between anchors, distance of anchors to the edge, anchor diameter and depth (Higgins and Klingner 1998; Gross et al. 2001; Cook and Konz 2001; Eligehausen and Cook 2006; Kim et al. 2013). Temperature has also been shown to determine anchorage capacities (Richardson et al. 2019, Hlavička and Lublóy 2018, Ba et al. 2021).

Cook and Konz (2001) conducted anchor tensile tests at two different temperatures, room temperature and 43˚C, to determine the effect of chemical anchors on bond strength (Cook and Konz 2001). Pinoteau et al. (2011) examined the tensile performance of anchors for different temperatures. They determined that there was no change in the tensile strength of the anchor at low temperatures. They observed that the anchor rods were directly affected, but there was no significant reduction in the tensile strength of the anchor at conditions above 20°C. They stated that the effect of heat should also be considered when designing shallow anchors (Pinoteau et al. 2011). The types of collapse in chemical anchors are steel rupture, concrete cone collapse and concrete splitting. The anchorage loses its strength in one or a combination of these situations (Bajer and Barnat 2012, Kim et al. 2013, Gonzalez et al. 2018). Concrete cone collapse depends on concrete properties, anchorage type and embedment depth (Yılmaz et al. 2013, Mcvay et al. 1996). Splitting of concrete depends on the concrete strength, the thickness of the element where the anchor is inserted and the distance of the anchor from the edge (Bajer and Barnat 2012). The stiffness of the anchor is less in cracked concrete compared to uncracked concrete. Cracks in concrete tend to loosen the interlock between the adhesive and concrete (Eligehausen and Balogh 1995). With the increase in material diversity, fiber reinforced (FRP) (Zhang et al. 2017, Li et al. 2018), carbon fiber reinforced (CFRP) (Wang et al. 2021, Sun and Ghannoum 2015), basalt fiber reinforced (BFRP) (Ma et al. 2019, Henin et al. 2019, Li et al. 2020) and glass fiber reinforced polymers (GFRP) (Maranan et al. 2015, Rosa et al. 2021). Anchors are also added to fiber-reinforced and self-compacting concretes other than normal concretes (Hamad et al. 2017, Nilforoush et al. 2017). They found that the addition of steel fibers improved the behavior of concrete up to 53% depending on the type of concrete and was effective in preventing the concrete from bursting (Kalthoff and Raupach 2020). When the studies were analysed, it was seen that the hole diameter to be drilled for planting the anchors was selected 4-8 mm more than the rod diameter (Yilmaz et al. 2013, Çalışkan and Aras 2017, Müsevitoğlu et al. 2020). However, it was stated that the hole diameter was not very effective in the performance of the anchor (Müsevitoğlu et al. 2020).

While determining the parameters in the study, the environmental conditions, diameters and depths encountered in the application area were taken into consideration. The diameter of the hole to be drilled was also determined by considering the studies conducted. When the literature is examined, it is seen that environmental conditions have not been addressed comprehensively. In this study, the tensile behavior of anchors under adverse conditions that may occur at different installation times was investigated. In the study, 6 different ambient conditions, 3 different diameters and 4 different planting depths were selected as variables. The behavior of individual chemical anchors planted in different diameters, depths and ambient conditions under tensile loads was investigated and safety levels were determined by evaluating according to the formulation in ACI 318 Annex-D Building Code Requirements for Structural Concrete: Anchorage to Concrete (ACI 318-19). Ribbed rods of 12, 16 and 20 mm B420C class were selected as diameter. Anchor rods were sown at 5, 10, 15 and 20 times the diameter

and in clean, semi-clean, humid, semi-humid, 50 and 150˚C ambient conditions. Unreinforced concrete elements with an average 28-day compressive strength of 21 MPa were used to plant the anchor rods. The holes where the rods were planted were drilled 4 mm more than the reinforcement diameter. For planting the anchor rods, a two-component, cartridge product, which is frequently used in the market for sprout planting, was selected. Pull-out tests were performed on 72 planted anchor rods and load-displacement graphs were obtained. Axial bearing capacity, failure modes, initial stiffnesses, displacement ductility ratios and energy consumption capacities were determined using the load-displacement graphs. Capacity and design strengths were calculated for the parameters used in the study according to the formulations in ACI 318 Appendix-D and compared with the experimental results.

2. Experimental study

The axial tensile capacities of chemical anchors and the failure load are related to the mechanical properties of the material, anchor diameter, embedment depth, drilled hole diameter, distance between anchors, distance of anchors from the edge. When adding new structural elements to existing structural systems, 12-, 16-, and 20-mm diameter rods and embedment depths consistent with the cross-sections of the structural elements are typically used. In this study, the effects of adverse conditions on chemical anchors were investigated. Anchor rods with diameters of 12, 16 and 20 mm are embedded at aspect ratios such as 5, 10, 15 and 20.

Environmental conditions anchor holes; Clean; It cleaned at least 3 times with the help of a compressor, Semi-clean; It cleaned once with the help of a compressor. Humidity, anchor holes saturated with water and waited for 12 hours and the water drained, semi-wet conditions, saturated water, waited for 1 hour and discharged the water were studied. Similarly, the environmental conditions where the anchor holes were heated to 50°C and 150°C. In this study, 72 anchor tests were applied. All these anchors were sealed with a two-component cartridge adhesive. Loads and displacements were measured during the experiments and load-displacement curves were plotted. From these curves, ultimate load capacities, initial stiffness, displacement ductility ratios, and energy absorption capacities were determined. The design forces of the ACI 318-19 anchors were compared to their axial tensile capacities. In addition, the safety coefficients were detected and the failure modes determined according to ACI 318 (Figure 1).

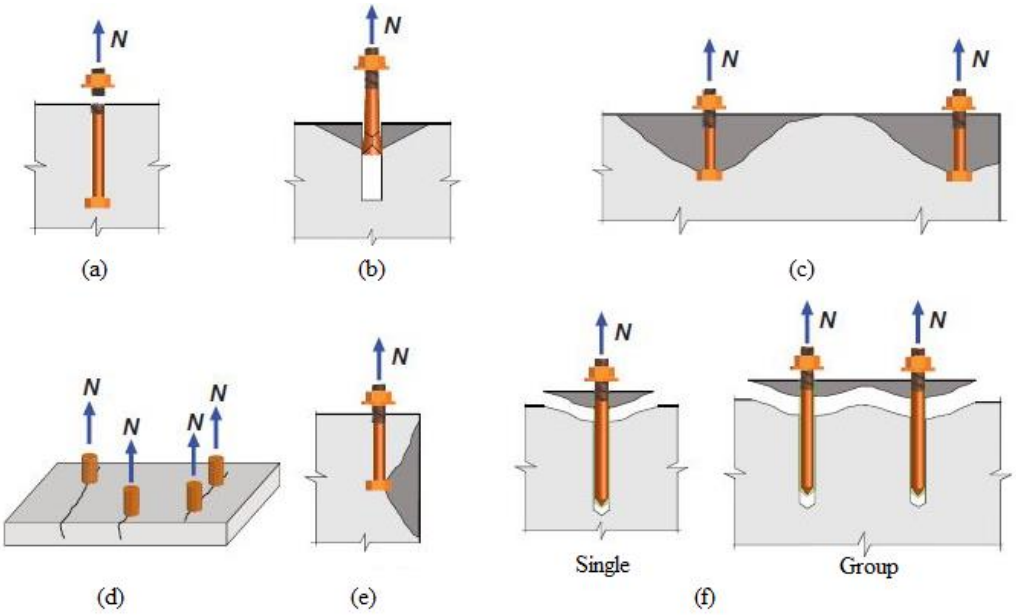

Figure 1. Anchor failure mechanisms, a-steel failure, b- pullout, c- concrete breakout, d- concrete splitting, e-side-face blowout, f-bond failure (ACI 318-19).

The strength of the chemical anchors, the quality of the concrete to be anchored, the depth of anchoring, the distance between anchors, the distance from the edge of the anchor, the diameter of the anchor hole, the ambient temperature, the preparation and application of the anchor holes, etc. are all factors that affect the strength. In this study, the distance between chemical anchors and anchor edge distances were incorporated in accordance with ASTM E-488 and, thus it was aimed to prevent edge failure or concrete cones to be affected by each other (Table 1).

Table 1. Anchor spacing and edge spacing (ASTM E-488).

	Chemical anchors	
Embedment length (l_d)	Distance between to anchors	Distance to edge and loading frame
<6d_0 (shallow)	2 l_d	1 l_d
6d_0-8d_0 (standard)	1,5 l_d	1 l_d
>8d_0 (deep)	1 l_d	0,75 l_d

The diameter of the drilled hole was created to be 40 mm larger than the diameter of the anchor reinforcement to be used. The fabrication and pull-out tests of the anchors were performed under various specified conditions. In the anchorage experiments, ribbed B420C rods were used. The tensile test was applied to the rods three tests of each diameter and the results were given in Table 2.

Table 2. Anchor mechanical properties.

Diameter (mm)	Average Yield strength (N / mm^2)	Average tensile strength (N / mm^2)	Elongation at break (%)
12	465	543	31
16	473	579	29
20	477	582	30

Concrete blocks produced as ready-mixed unreinforced concrete of class C20/25. The mixing ratios by weight of the concrete was shown in Table 3. A pressure test was performed on day 28 on the three samples taken during production. The results were shown in Table 4. Anchor rods embedded using epoxy. Table 5 was given the properties of the epoxy-based adhesive.

Table 3. Mixing ratios by weight for 1 m^3 of concrete.

Material	C 20/25 (kg)
0-4 mm	1180
5-12 mm	225
12-22 mm	510
CEM I 42.5	260
Water	190
Chemical	3.5

Table 4. 28-day concrete compressive strength.

C 20/25 (MPa)			
I	II	III	Average
21.25	21.73	20.13	21.04

Table 5. Mechanical properties of chemical adhesive.

Material structure	
Component	2
Mixing ratio	A: B = 10:1
Colour	Grey
Compressive Strength	83 MPa (ASTM D 695)
Bending Strength	29 MPa (ASTM D 790)
Tensile Strength	15 MPa (ASTM D638)
Elastisite Modülü	3800 MPa (ASTM D 638)
Density	1.8 kg/l

In this study, 12-, 16-, and 20-mm diameter anchor rods were used. Depths of 5, 10, 15, and 20 times the diameter were chosen as embedment depths. Clean/semi-clean, wet/semi-wet, and 50°C/150°C ambient conditions were variably examined in the study. Variations and explanations of the variables were presented and explained in Table 6. In this study, a two-component product, cartridges, widely used in the market, was used to embed the anchors. This material is a two-component, fast-curing product used to embed high-performance anchor rods. It is a cartridge product and is widely used for sprouting.

Table 6. The parameters used in the study.

Specimen		Diameter (mm)	Aspect ratio (h_{ef}/d)	Explanation
C	Clean			The situation that the anchor holes are completely purified from dust. Cleaning with the help of a compressor at least 3 times.
SC	Semi-Clean	12	5	The situation that the anchor holes are left dusty. Cleaning with the help of a compressor only once.
H	Humidity	16	10	The anchor holes are saturated with water and waited for 12 hours and the water is drained.
SH	Semi-Humidity	20	15 20	The anchor holes are saturated with water and waited for 12 hours and the water is drained.
50°C	50°C			The situation of embedding rods by heating to 50°C from the inner surface of the anchor holes.
150°C	150°C			The situation of embedding rods by heating to 150°C from the inner surface of the anchor holes.

The holes for the anchors were drilled considering the distance between the anchors and according to the edge boundary conditions given in ASTM E-488-5 Regulation. Hole diameters were selected 4 mm larger than the diameter of the anchor rod to be erected. The 72 holes were cleaned from dust with the help of compressed air. 12 anchor holes were not cleaned

completely and left dusty. B420C ribbed bars were sewn into the drilled holes using chemical adhesive. Care was taken to ensure that there were no air bubbles, that they were placed perpendicular to the base concrete and that they were protected until the adhesive set.

In order to determine the tensile strength of 72 anchors embedded in different settings on concrete blocks, they were given in Figure 2, and the pull-out test was done. The test set consists of a hydraulic piston to apply tensile force to the anchors, a load cell to measure the forces, a displacement gauge to measure the amount of displacement, a steel block used to see the type of failure, a data collection device to take the measurements, and a toothed jaw to hold the anchor rods. The anchor rods held by the threaded jaws were pulled with a hydraulic piston, and measurements were taken with a load cell and displacement meter, and load-displacement curves were obtained. The schematic representation of the experimental setup used in the study was given in Figure 3.

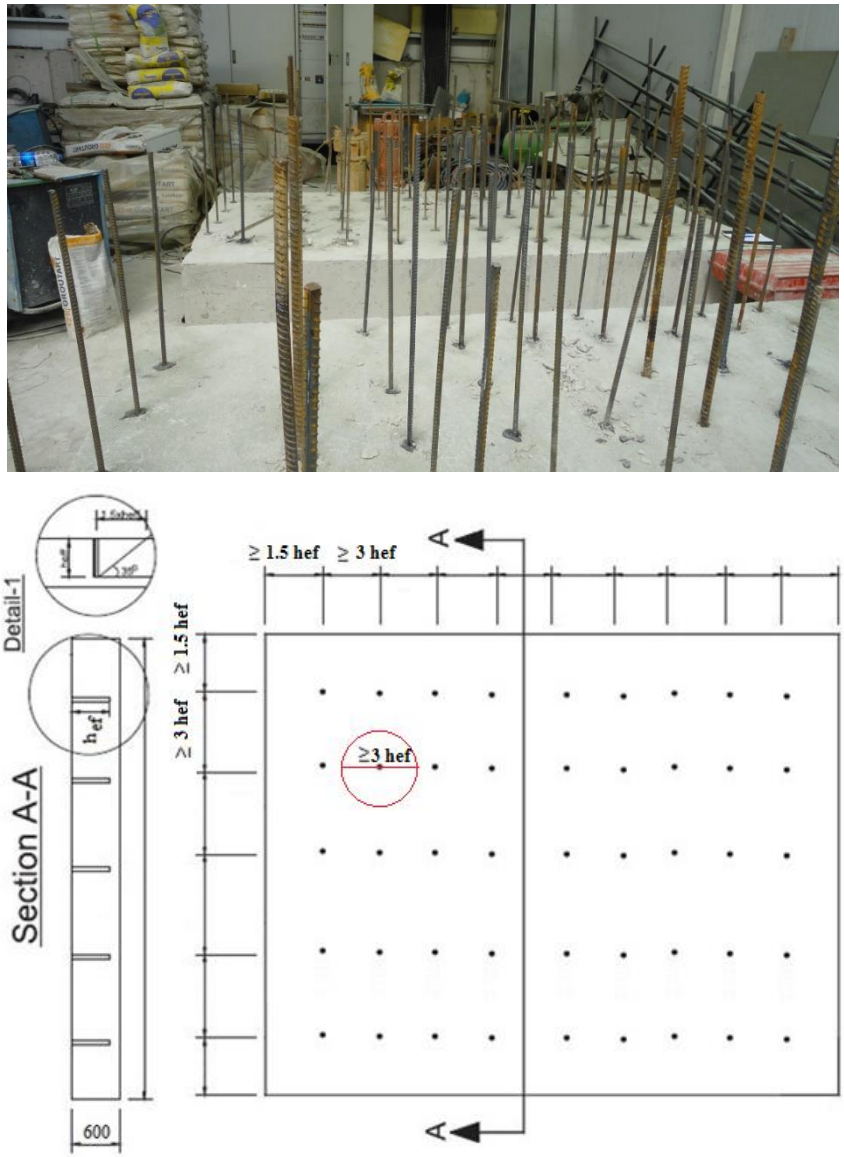

Figure 2. Experimental concrete blocks.

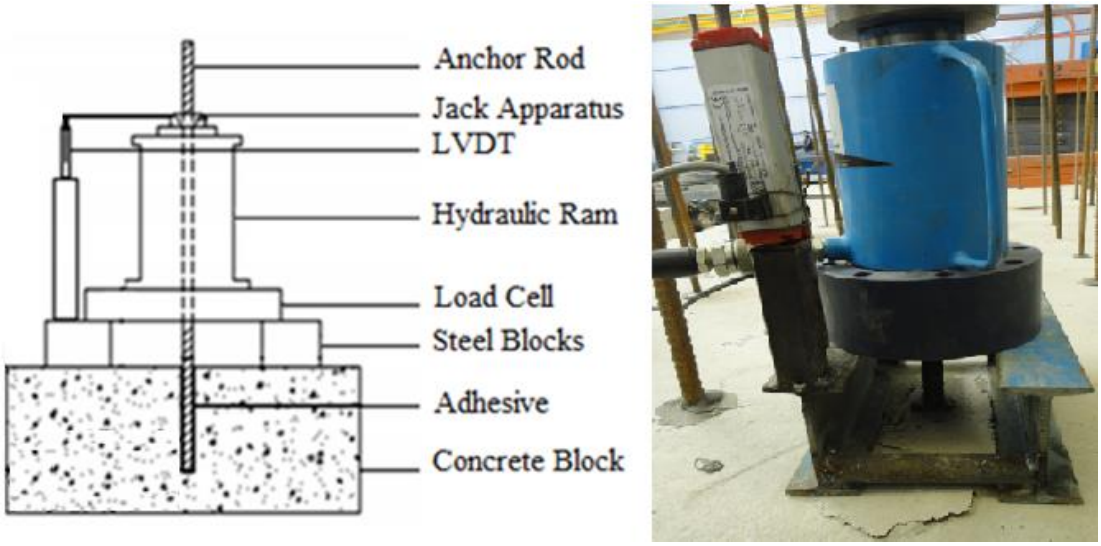

Figure 3. Test and experimental setup.

Formulas for determining the design and capacity strength of chemical anchors under tensile forces are given in ACI 318-19 according to failure modes (steel failure, pullout, concrete cone capacities). The formulation includes failure modes, anchor diameter, embedment depth, edge spacing, quality of workmanship and strength reduction coefficient according to the effect of ambient conditions. In the known literature, there is no formula-tion including humidity, dust and temperature conditions. The tensile strengths obtained in the experimental results, capacity, design strength and safety levels were determined in accordance with ACI 318-19. Tensile strength in the proposed formulation; steel failure, concrete cone and stripping capacities were calculated separately. ACI 318 suggested axial tensile capacities;

Capacity building;

$$N_{sa} = nA_{se}f_{uta} \quad (1)$$

$$A_{se} = \frac{\pi}{4}\left(d_a - \frac{0{,}9743}{n_t}\right)^2 \quad (2)$$

where, n is the number of anchor, A_se is the effective cross-sectional area and f_uta is the ultimate strength (f_uta< min (1.9f_ya) or 860 MPa). Concrete cone capacity

For single anchor;

$$N_{cb} = \frac{A_{Nc}}{A_{Nco}}\Psi_{ed,N}\Psi_{c,N}\Psi_{cp,N}N_b \quad (3)$$

where, A_{Nc} is the estimated failure area in concrete, A_{Nco} is the estimated the failure area in 1.5 h_{ef} edge distance, N_b is the nominal concrete failure strength, $\Psi_{ed,N}$ is the reduction coefficient for distance to free edge and $\Psi_{c,N}$ is the reduction coefficient for cracked and uncracked concrete.

For post-added anchors, the nominal resistance to concrete failure can be calculated based on a certain coefficient.

$$N_b = k_c\lambda_a\sqrt{f_c'}h_{ef}^{1,5} \quad (4)$$

The anchor under tensile force must not exceed the breaking strength N of the concrete. Where, k_c are the coefficients 17, 10 and for the chemical ankraj, pre-installed and installed anchor bolt respectively, also k_c is a factor evaluated for experimental data at 5% fractile as per ACI 318 and ACI 355. The coefficients given in the equation must be determined according to the edge spacing.

If $c_{a,min} \geq 1{,}5\ h_{ef}$, then $\Psi_{ed,N} = 1$

If $c_{a,min} \leq 1{,}5\ h_{ef}$, then $\Psi_{ed,N} = 0{,}7 + 0{,}3\ \frac{c_{amin}}{1{,}5 h_{ef}}$

The capacity and design strength values according to the failure modes given in ACI 318-19 for the parameters used in the study are given in Table 7. The strength reduction coefficient is 0.50 considering the unreinforced concrete, which is highly affected by the quality of workmanship and ambient conditions and has low reliability.

Table 7. ACI 318 capacity and design strength values.

Diameter (mm)	Embedment depth (mm)	Steel capacity	Cone capacity	ACI capacity Strength (kN)	ACI design Strength (kN)
12	60	65.10	23.87	23.87	11.94
	120		42.28	42.28	21.14
	180		61.99	61.99	31.00
	240		77.37	65.10	32.55
16	80	115.70	29.89	29.89	11.94
	160		55.38	55.38	21.14
	240		77.37	77.37	31.00
	320		100.03	100.03	32.55
20	100	115.70	29.89	29.89	14.95
	200		55.38	55.38	27.69
	300		77.37	77.37	38.69
	400		100.03	100.03	50.02

2.1. *Initial stiffness, displacement ductility ratio and energy absorption capacity*

2.1.1. Initial stiffness

Stiffness is the parameter that determines the displacement of a material, element or struc-ture under a certain load. The stiffness of the combination of concrete, chemical adhesive and reinforcement used for anchoring is the slope of the line drawn on the load-displacement curve (Ki). The initial stiffness is given in Figure 4. The initial stiffness gives information about the behavior of the system and is used as a characteristic parameter in analytical studies.

2.1.2. Displacement ductility ratio

Ductility is the ability of a system or an element to flex without losing its bearing capacity. The ductility ratio in chemical anchor application is determined according to the types of failure, taking into account the load-displacement curves. In specimens with loss of strength, the failure ratio is the deflection value corresponding to the load value that is 0.85 times the maximum load on the load-displacement curve. In specimens with increased strength, the failure rate is the displacement at the failure point. The reinforcement to yield ratio is the deflection value corresponding to the maximum load. The ductility ratio was obtained by proportioning the value of displacement at failure to the value of displacement at yield (δ_f/δ_{max}). The point at which it began to leaf out was also considered in specimens exhibiting failure -type leaf out. A large ductility capacity means that the system or element can absorb large energy. Considering that the earthquake is an energy loading, the ductility will absorb the energy while the earthquake is loading energy.

2.1.3. Energy absorption capacity

The energy absorption capacity is obtained by finding the shaded area under the load-displacement curve obtained during the experiment (Figure 4). The energy absorption capacity gives information about the performance of the system.

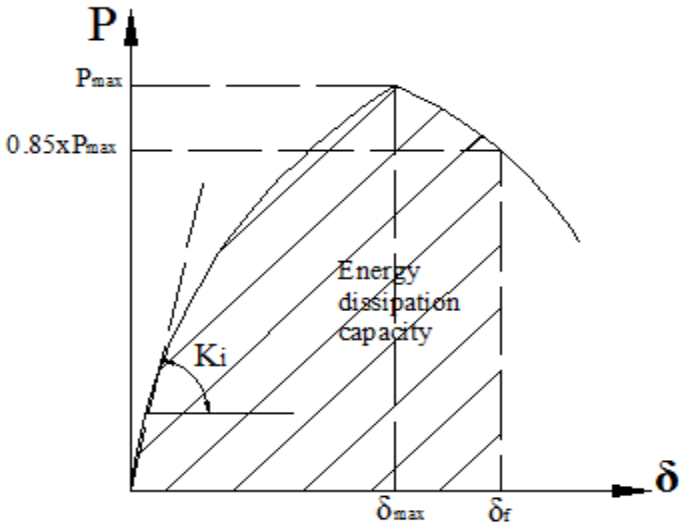

Figure 4. Calculation of values from the load-displacement curve.

3. Experimental results and discussion

In this chapter, the load-displacement curves, stiffness, displacement ductility ratios, energy absorption capacities, failure types, and safety coefficient values according to ACI 318 obtained from pullout tests on anchor rods embedded in different diameters, embedment depths, and environmental conditions. In the experimental study, a total of 72 pull-out tests were performed. The test program consists of 2x12 tests for clean and semi-clean conditions, 2x12 tests for wet and semi-wet conditions, and 2x12 tests for temperature conditions of 50°C-150°C. The names of the test items were summarized in Table 5. The general load-displacement behavior graphs obtained from the experimental study was shown in Figure 5. The anchor elements were pulled out prior to yield for embedment depths 5 and 10 under semi-clean, wet, 150°C ambient conditions. The anchor elements were considered yielding for embedment depths 15 and 20 under full ambient conditions. In addition, the elasticity ranges become more noticeable. The shallow embedment depths and ambient conditions were established to be more effective in the anchoring elements.

3.1. Cleaning condition: tensile strength values and failure modes for cleaning and semi-cleaning conditions

The condition of cleaning the open anchor holes with a compressor at least 3 times is clean, and the single cleaning condition is semi-clean. In the following comments of the experimental study, the experimental items in the clean condition will be interpreted as reference experiments. An axial tensile force was applied to the embedded anchors and load-displacement graphs were obtained. Figure 6 shown the failure mechanism for some of the tested specimens. From these curves, the tensile strength, initial stiffness, displacement ductility ratio, energy absorption capacity and failure modes of the anchors were determined (Table 8). The initial stiffness, displacement ductility ratio, and energy absorption capacity obtained from the load displacement curve resulted in reductions in the semi-clean condition. This shows that when the test elements are semi-clean, it leads to a decrease in ductility. When the load displacement curves of chemical anchor elements embedded in a clean and dusty environment were examined, it was observed that the initial stiffness, displacement ductility rate and energy absorption capacity were decreased in the clean environment.

Among the cleaning test elements, the maximum axial tensile capacity was obtained at 139.5 kN in test element CD20L40. When evaluated in terms of anchor diameters of 12, 16, and 20 mm, the average tensile strength values of the anchors are 43, 77, 132 kN and 37, 66, 123 kN for the clean and semi-clean conditions, respectively. Looking at Figure 7, it can be seen that

the axial tensile capacities increase with increasing anchor diameter and embedment depth in general. In the first 24 experimental elements, peeling is generally observed as the failure mode. Axial tensile forces increase with increasing anchor diameter and embedment depth. A decrease in axial tensile capacity was observed when cleaning the anchor hole to the intended level. The axial tensile capacities of the 12-, 16-, and 20-mm anchor rods decreased by an average of 14, 12, and 7 percent, respectively.

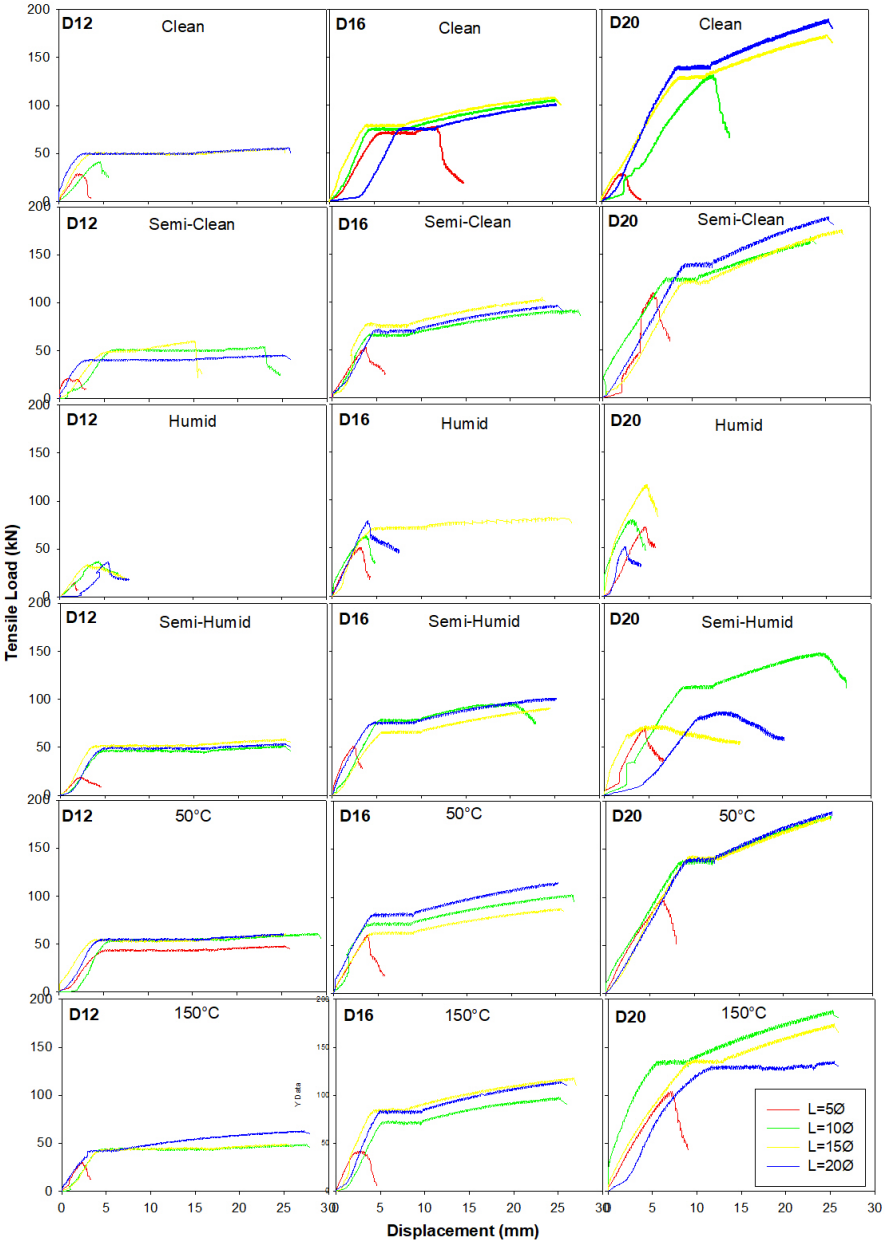

Figure 5. Load- displacement relationships test specimens.

3.2. Humidity condition: tensile strength values and failure modes for wet and semi-wet conditions

The open anchor holes were filled with water completely, and the condition of waiting 24 hours to be emptied was wet, and when the same process took place in 1 hour, a semi-wet condition was created. The results obtained were given in Table

9. The maximum axial tensile capacity among the test elements in wet condition was obtained as 107 kN in the test element SHD20L40, were given in Figure 8. When evaluated in terms of anchor diameter of 12, 16 and 20 mm, the average tensile strength values of the anchors are 30, 66, 87 kN and 41, 67, 93 kN for wet and semi-wet conditions, respectively. When examining the load-displacement curves of chemical anchors embedded in wet and semi-wet environment, it was found that the initial stiffness, displacement ductility ratio and energy absorption capacity of the anchors presented in the semi-wet environment were reduced.

Figure 6. Image for the test samples (CB: concrete breakout, P: pull-out).

Table 8. Cleaning status: test and calculation results for clean, semi-clean.

Anchor diameter (mm)	Embedment depth (mm)	Tensile strength (kN) C-SC		Initial stiffness K (kN/mm) C-SC		Displacement ductility ratio C-SC		Energy dissipation capacity (kN mm) C-SC		Experimental failure mode C-SC	
12	5Φ	29.3	21.4	14.37	20.0	1.36	2.12	32.35	24.26	CB	CB
	10Φ	41.7	40.3	9.37	8.80	1.06	3.40	65.00	494.40	CB	CB+P
	15Φ	49.8	48.1	14.10	9.77	4.64	1.78	476.16	186.14	P	CB+P
	20Φ	49.8	38.1	18.51	14.47	5.87	5.56	441.56	346.31	P	P
16	5Φ	77.9	52.7	6.57	13.83	1.05	1.05	389.45	74.46	CB+P	CB
	10Φ	73.9	64.5	15.96	15.25	1.97	2.05	316.46	272.47	P	P
	15Φ	79.6	77.5	17.97	19.38	1.94	2.15	272.02	323.16	P	P
	20Φ	74.9	68.5	9.59	14.60	1.51	1.97	241.70	299.90	P	P
20	5Φ	29.1	110.3	12.00	19.56	1.12	1.09	22.44	168.40	CB	CB
	10Φ	131.5	124.7	10.55	17.03	1.05	1.44	518.81	604.60	P	P
	15Φ	126.4	121.1	14.73	13.27	1.34	1.30	595.03	629.33	P	P
	20Φ	139.5	135.0	16.41	14.10	1.46	1.30	701.67	650.45	P	P

CB: Concrete breakout, P: Pull-out.

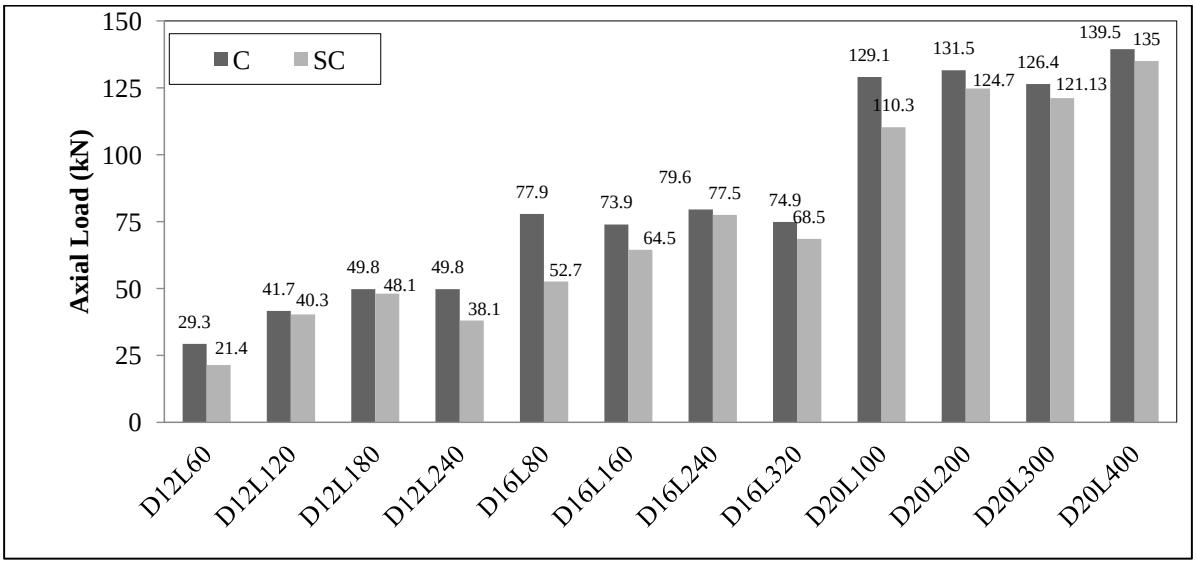

Figure 7. Maximum axial tensile capacities for clean-semi-clean conditions.

Table 9. Humidity condition: test and calculation results for humid/semi-humid.

Anchor diameter (mm)	Embedment depth (mm)	Tensile strength (kN) H-SH		Initial stiffness K (kN/mm) H-SH		Displacement ductility ratio H-SH		Energy dissipation capacity (kN mm) H-SH		Experimental failure mode H-SH	
12	5Φ	14.7	18.8	9.03	8.09	1.07	1.17	8.52	20.75	CB	CB
	10Φ	36.9	45	8.38	4.41	1.13	3.6	64.69	374.55	CB	P
	15Φ	33.7	51.2	10.73	13.82	1.7	4.06	75.44	323.74	CB	P
	20Φ	36.4	49.5	6.78	10.04	1.04	3.52	39.13	568.26	CB	P
16	5Φ	50.7	51.5	16.21	21	1.12	1.09	66.91	59.08	CB	CB
	10Φ	62.8	78.3	16.52	14.66	1.08	1.87	99.27	355.57	CB	CB+P
	15Φ	70.3	64.6	15.72	11.66	2.36	1.81	437.56	295.33	P	P
	20Φ	78.3	73.9	19.63	17.44	1.07	2.14	106.4	350.02	CB	P
20	5Φ	71.9	79.6	15.54	15.53	1.05	1.07	114.22	99.21	CB	CB
	10Φ	79.5	82.8	26.52	12.85	1.37	1.38	141.82	516.71	CB	CB+P
	15Φ	95.8	103.2	24.73	12.68	1.15	1.77	257.16	373.86	CB	CB
	20Φ	101.3	107.3	21.55	6.34	1.08	1.24	34.18	488.67	CB	CB

CB: Concrete breakout, P: Pull-out.

When examining the experimental elements, a decrease in the tensile forces of the reference anchor was found under wet and semi-wet conditions. In addition, humidity in the anchor holes, or in other words, increasing the time of exposure to water, leads to a decrease in the axial tensile capacity. In the experimental group, debonding is generally observed in the experimental element as a failure mode. The axial tensile capacities of the 12-, 16-, and 20-mm anchor rods were reduced by 18, 14, and 34% for the wet condition and 5, 13, and 30% for the semi-wet condition, respectively, compared to the reference test elements (Figure 8).

3.3. Temperature condition: tensile strength values and failure modes for the 50°C-150°C condition

The drilled anchor holes were heated to 50°C and 12-, 16- and 20-mm diameter anchor rods were driven to a depth of 5, 10, 15 and 20 times the diameter. Table 10 shown the results obtained. When the test elements were examined, reductions occurred from the reference anchor forces in both the 50°C and 150°C cases. In addition, the increase in temperature in the anchor holes creates a decrease in axial tensile capacities. In the experimental group, scraping is generally considered a no-madic mode in the experimental element. The average axial tensile capacities at 50°C and 150°C for 12-, 16-, and 20-mm anchor bars in the experimental elements were obtained as 48, 73, 127 kN and 39, 70, 124 kN respectively. With the increase in temperature, the axial tensile capacities decreased by 19, 4.3%, respectively. The average axial tensile capacities decreased by +4%, 5, 3 and 7%, 9.5% respectively for temperatures of 50°C and 150°C in the 12-, 16- and 20-mm anchors according to the reference (Figure 9).

Table 10. Temperature status: test and calculation results for 50 °C-150 °C status.

Anchor diameter (mm)	Embedment depth (mm)	Tensile strength (kN) 50°C-150°C		Initial stiffness K (kN/mm) 50°C-150°C		Displacement ductility ratio 50°C-150°C		Energy dissipation capacity (kN mm) 50°C-150°C		Experimental failure mode 50°C-150°C	
12	5Φ	32.3	29	8.68	13.31	3.73	0.83	421.53	28.09	P	CB
	10Φ	51.8	42.1	9.48	9.81	3.43	4.02	531.63	418.67	P	P
	15Φ	53.3	41.1	13.74	9.92	4.06	4.4	489.21	428.75	P	P
	20Φ	53.3	42.1	12.01	13.66	3.82	3.8	483.01	276.13	P	P
16	5Φ	60.7	42	15.51	19.74	1.03	1.16	82.4	61.58	CB	CB
	10Φ	69.9	72.4	18.54	7.56	2.34	1.84	404.41	293.42	P	P
	15Φ	80.8	82.4	14.24	18.47	2.11	1.02	274.63	303.14	P	P
	20Φ	82.3	81.3	18.44	15.9	2.04	1.89	371.96	349.07	P	P
20	5Φ	98.9	104.2	15.47	14.83	1.12	1.09	470.64	285.3	CB	CB
	10Φ	134.	133.1	15.63	23.27	1.4	1.59	704.23	600.42	P	P
	15Φ	139.	132.9	14.64	14.48	1.39	1.41	764.9	777.1	P	P
	20Φ	136.	126.6	14.72	11.25	1.33	1.56	658.4	977.38	P	P

CB: Concrete breakout, P: Pull-out.

As a result of the load displacement curves of chemical anchors, it was observed that the initial stiffness, displacement ductility ratio and energy consumption capacity of all anchors. Averages of initial stiffness, displacement ductility and energy consumption capacity in embedded anchors in clean and semi-clean environment were 13.35 kN/mm, 15 kN/mm, 2.03, 2.1 and 339 kN.mm, 339.5 kN.mm, respectively (Figure 10, 11). In this situation, it was observed that the tensile forces decreased and caused a large displacement in the embedded anchors in the dusty environment.

The average initial stiffness, displacement ductility, and energy consumption capacity of anchors embedded in a wet and semi-wet environment were 16 kN/mm, 12 kN/mm, 1.26, 2.1, and 120 kN.mm, 319 kN.mm, respectively (Figure 10, 11). In this case, anchors embedded in a semi-wet environment were superior in terms of tensile strength and energy consumption compared to anchors embedded in a wet environment.

In the anchors embedded in 50°C and 150°C environment, the averages of initial stiffness, displacement ductility and energy consumption capacity were obtained as 14 kN/mm, 14 kN/mm, 2.3, 2.1 and 471 kN.mm, 400 kN.mm respectively (Figure 10, 11). In this occasion, anchors embedded in 50°C environment were superior in terms of tensile strength and energy consumption compared to anchors embedded in 150°C environments.

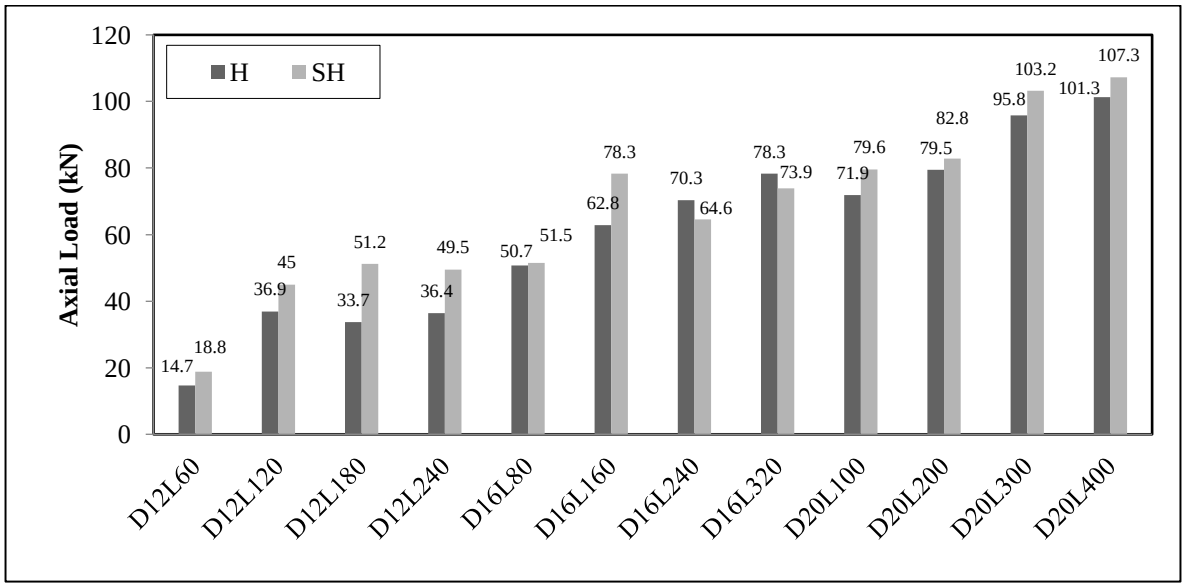

Figure 8. Maximum axial tensile capacities for humid-semi humid conditions.

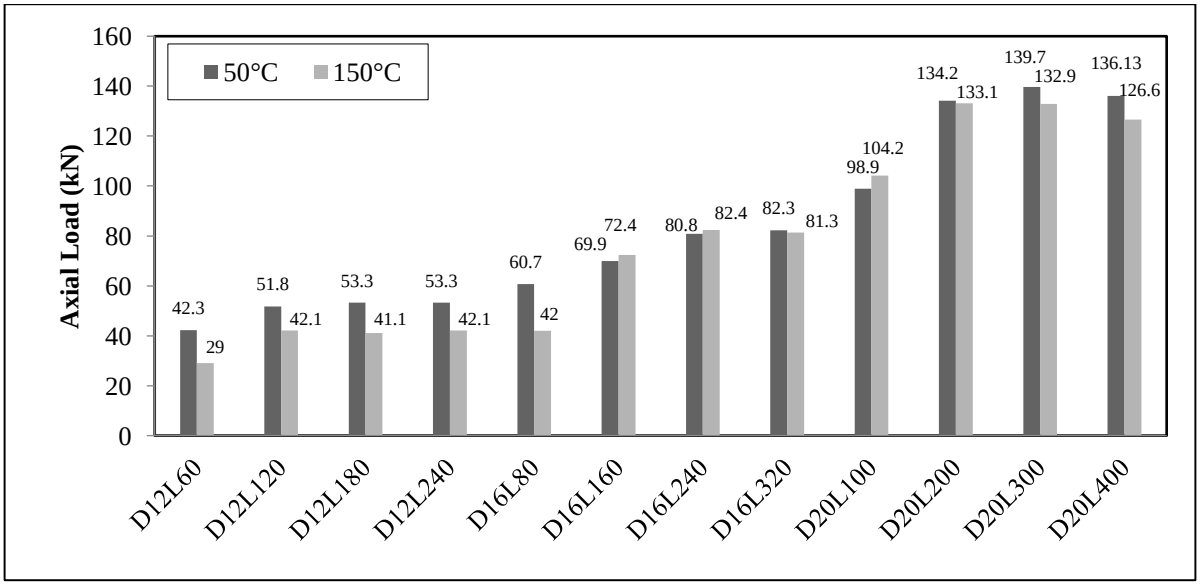

Figure 9. Maximum axial tensile capacities for 50°C and 150°C situations.

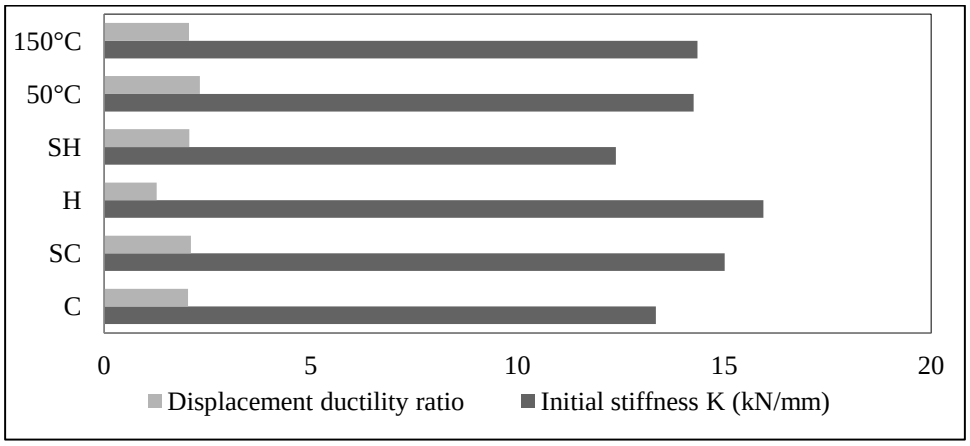

Figure 10. Initial stiffness and displacement ductility ratio.

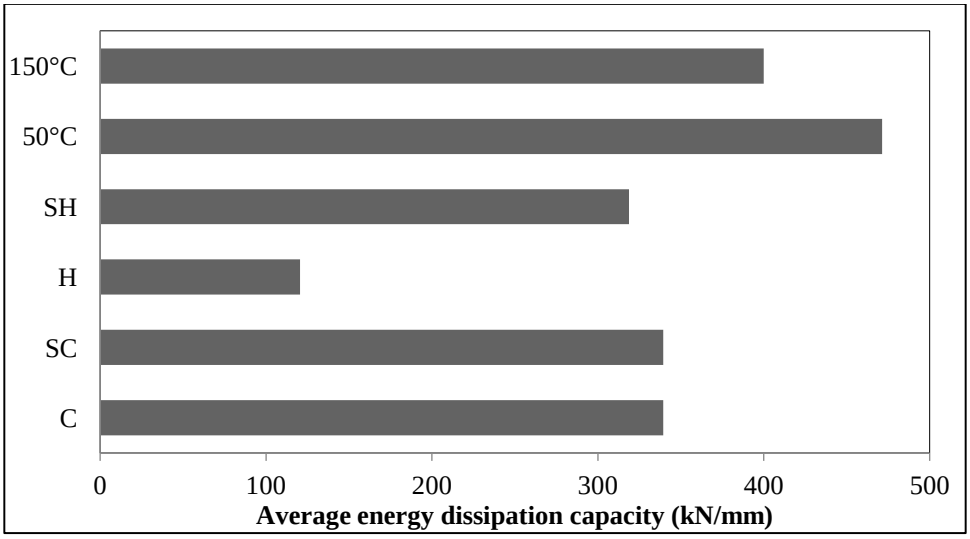

Figure 11. Average energy dissipation capacities (kN/mm).

3.4. Evaluation for anchor bars with a diameter of 12 mm

Tensile forces obtained from testing anchor bars with a diameter of 12 mm under seven different environmental conditions were obtained. Compared to the tensile forces of anchor rods embedded in a clean and semi-clean environment, reductions of 27, 4, 4 and 24% respectively with increasing embedment depths were obtained. Compared to the values of anchor bars embedded in a wet and semi-wet environment, a decrease of 22, 18, 34 and 27% was determined with increasing embedment depths, respectively. Compared to the values of anchor bars embedded in 50°C and 150°C environment, there was a decrease of 31%, 19, 23 and 21% respectively with increasing embedding depths.

3.5. Evaluation for anchor bars with a diameter of 16 mm

Tensile force values obtained from testing anchor bars with a diameter of 16 mm under seven different environmental conditions were obtained. Compared to the tensile forces of anchor bars embedded in a clean and semi-clean environment, the embedment depths decreased by 32, 13, 3 and 9%, respectively. Comparing the values of the embedded anchor bars in wet and semi-wet environment, the embedding depth increased, and the embedded rods in 240 mm depth increased by 8% and the embedded rods in 320 mm depth increased by 6%. Compared to the values of the embedded rods in a 50°C and 150°C

environment, there was a 31% decrease for the rods embedded in a depth of 80 mm and 1% for the rods embedded in a depth of 320 mm.

3.6. Evaluation for anchor bars with a diameter of 20 mm

The tensile forces obtained from testing anchor bars with a diameter of 20 mm under seven different environmental conditions were obtained. Compared to the tensile forces of anchor bars embedded in a clean and semi-clean environment, a decrease of 15, 5, 4 and 3% respectively with increasing embedment depth is observed. Compared to the values of anchor bars embedded in wet and semi-wet environment, a decrease of 30, 4, 7 and 6% was determined by increasing the embedding depths.

When the experiments regarding the cleaning condition are considered in terms of ACI 318 safety levels, it can be seen that the cleanliness of the anchor holes exceeds the safety factor. In cases where the cleaning requirement is not met in the experimental elements, it is seen that the safety levels remain at a risky level. This situation again shows that the cleaning parameter must be considered in anchoring applications. When the experiments for humidity are considered in terms of ACI 318 safety levels, it can be seen that the exposure of anchor holes to humidity 24 hours a day is low in safety factor. Compared to the baseline results in the experimental elements, it was observed that the safety levels decrease. When the safety levels of 50°C and 150°C were considered, it was observed that the temperature increase and the safety coefficient decreased. Figure 12 shown the safety levels of the experimental elements, is examined, generally the adverse environmental conditions prevent them from achieving the targeted performance levels.

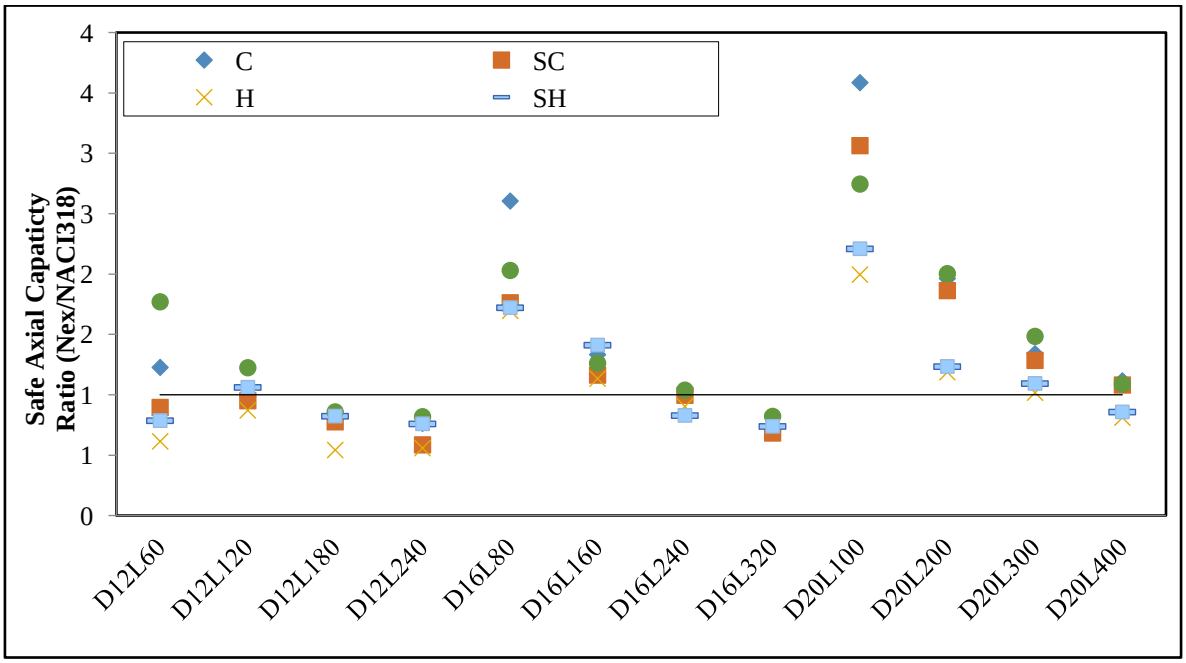

Figure 12. Safety levels according whole conditions.

4. Conclusions and comments

In this study, 12-, 16-, and 20-mm diameter anchor bars were embedded under clean, semi-clean, wet, semi-wet conditions at 50°C and 150°C, at depths of 5, 10, 15, and 20 times the diameter, and exposed to a pull-out test. The result of these experiments provided load-displacement curves of the anchor bars. The final tensile force values, initial stiffnesses, displacement ductility ratio, energy absorption capacities and failure modes were determined from the load-displacement curves. In addition, coefficients of safety were determined by comparing the design capacity and strength values using ACI 318 for chemical anchors. The results obtained in this study can be listed as follows.

1. Regardless of the ambient condition, the tensile force increased as the anchor diameter increased. The average tensile force values of the specimens with clean ambient condition; There was an increase of 79% from 12 mm to 16 mm and 150% from 16 mm to 20 mm. In the semi-clean condition, these values increased by 68% and 214%, in the humid environment, there was an increase of 79% from 12 mm to 16 mm and 39% from 16 mm to 20 mm. For the samples with semi-clean ambient conditions, the average increase was 68% for 16 mm and 86% for 20 mm. The increases were 115% and 161% for humid condition, 63% and 27% for semi-humid condition, 36% and 85% for 50˚C condition, 80% and 79% for 150˚C condition.
2. Regardless of the ambient condition, the seeding depth generally increased up to 15Ø, after which it either decreased or increased slightly. In the clean condition, it increased 42% from 5Ø to 10Ø and 19% from 10Ø to 15Ø. In the case of semi-clean, humid and 150˚C; it increased up to a depth of 10Ø and then decreased. In the semi-moist and 50˚C cases, the tensile capacities increased up to a depth of 15Ø and then decreased.
3. In the experimental study (cleaning, humidity and temperature conditions), the worst-case condition was performed as a wet condition.
4. The average strength losses of the anchor bars during transitions from clean to dusty environments are 12%, 14% for 12 mm diameter anchors, 14% for 16 mm diameter anchors and 7% for 20 mm diameter anchors.
5. The average strength losses in the anchor bars during transitions from a semi-wet to a wet environment are 11%, 25% in 12 mm diameter anchors, 2% in 16 mm diameter anchors and 7% in 20 mm diameter anchors.
6. Anchor elements embedded in wet and semi-wet environments caused strength losses of 20% and 12%, respectively, according to reference testers.
7. The average strength losses in the anchor bars during transitions from 50°C to 150°C are 11%, 24% in 12 mm diameter anchors, 7% in 16 mm diameter anchors and 2% in 20 mm diameter anchors.
8. Anchor elements embedded in 50°C and 150°C environments resulted in strength losses of 6% with an increase of 3% respectively compared to the reference tests.
9. The maximum energy ingestion capacity is 50°C, and the minimum is reached in anchor elements embedded in a humid environment.
10. The test results were compared with the capacity and design strengths given in ACI 318-19 and the safety coefficients were determined. When all the test results were evaluated, the design strength safety numbers were above 1 regardless of the ambient conditions. More than 50% of the capacity strength safety values were below 1 for the specimens made for humid and semi-humid conditions. The average safety number for capacity strength was 1.2 for clean environment and 2.5 for design strength. For semi-clean condition it was 1.3-2.6; for moist condition it was 1-2; for semi-moist condition it was 1.1-2.2; for 50˚C condition it was 1.4-2.8; for 150˚C condition it was 1.3 for capacity strength and 2.6 for design strength. It is seen that the most unfavorable condition is humid and semi-humid condition.

In this study, it is found that the axial tensile strength decreases with different environmental conditions and periods of exposure to the situation. Therefore, it is necessary to take care of chemical anchoring applications in conditions such as dust, humidity and temperature.

Author contributions: This study is based on the master's thesis prepared by Yılmaz Ağdağ under the supervision of Dr. Özlem Çalışkan. The authors contributed to the conduct and interpretation of the experiments and the preparation of this article.

Funding: This research was supported by Agdag Construction.

Acknowledgments: The authors would like to thank Agdag Construction for their support in the production of the samples.

Conflicts of interest: The authors declare no conflicts of interest.

References

ACI 318. (2019). Building code requirements for structural concrete (ACI 318-19) and commentary. American Concrete Institute.

ASTM E488-96. (2003). Standard test methods for strength of anchors in concrete and masonry elements.

Ba, G., Weng, X., Liu, C., & Miao, J. (2021). Bond strength of corroded reinforcements in concrete after high-temperature exposure. Construction and Building Materials, 270, 121400.

Bajer, M., & Barnat, J. (2012). The glue–concrete interface of bonded anchors. Construction and Building Materials, 34, 267-274.

Bokor, B., Sharma, A., & Hofmann, J. (2022). Experimental investigations on the concrete edge failure of shear loaded anchor groups of rectangular and non-rectangular configurations. Experimental investigations on the concrete edge failure of shear loaded anchor groups of rectangular and non-rectangular configurations, 222, 111153.

Cook , R. A., & Konz, R. C. (2001). Factors Influencing Bond Strength of Adhesive Anchors. Factors Influencing Bond Strength of Adhesive Anchors, 98(1), 76-86.

Cook, R. A. (1993). Behavior of chemically bonded anchors. Journal of Structural Engineering, 119(9), 2744-2762.

Çalışkan, Ö., & Aras, M. (2017). Experimental investigation of behaviour and failure modes of chemical anchorages bonded to concrete. Construction and Building Materials, 156, 362-375.

Çalışkan, Ö., Yılmaz, S., Kaplan, H., & Kıraç, N. (2013). Shear strength of epoxy anchors embedded into low strength concrete. Construction and Building Materials, 38, 723-730.

Eligehausen , R., & Balogh, T. (1995). Behavior of Fasteners Loaded in Tension in Cracked Reinforced Concrete. Structural Journal, 92(3), 365-379.

Eligehausen, R., Cook, R. A., & Appl, J. (2006). Behavior and Design of Adhesive Bonded Anchors. ACI Structural Journal, 103(6), 822-831.

Epackachi, S., Esmaili, O., Mirghaderi, S. R., & Behbahani, A. T. (2015). Behavior of adhesive bonded anchors under tension and shear loads. Journal of Constructional Steel Research, 114, 269-280.

Gross, H. J., Klingner, R. E., & Graves, H. L. (2001). Dynamic Behavior of Single and Double Near-Edge Anchors Loaded in Shear. Structural Journal, 98(5), 665-676.

Hamad, R. J., Johari, M. M., & Haddad, R. H. (2017). Mechanical properties and bond characteristics of different fiber reinforced polymer rebars at elevated temperatures. Construction and Building Materials, 142, 521-535.

Henin, E., Tawadrous, R., & Morcous, G. (2019). Effect of surface condition on the bond of Basalt Fiber-Reinforced Polymer bars in concrete. Construction and Building Materials, 226, 449-458.

Higgins, C. C., & Klingner, R. E. (1998). Effects of Environmental Exposure on the Performance of Cast-In-Place and Retrofit Anchors in Concrete. Structural Journal, 95(5), 506-517.

Hlavička, V., & Lublóy, É. (2018). Concrete cone failure of bonded anchors in thermally damaged concrete. Construction and Building Materials, 171, 588-597.

Kalthoff, M., & Raupach, M. (2021). Pull-out behaviour of threaded anchors in fibre reinforced ordinary concrete and UHPC for machine tool constructions. Pull-out behaviour of threaded anchors in fibre reinforced ordinary concrete and UHPC for machine tool constructions, 33, 101842.

Kim, J.-S., Jung, W.-Y., Kwon, M.-H., & Ju, B.-S. (2013). Performance evaluation of the post-installed anchor for sign structure in South Korea. Performance evaluation of the post-installed anchor for sign structure in South Korea, 44, 496-506.

Li, T., Zhu, H., Wang, Q., Li, J., & Wu, T. (2018). Experimental study on the enhancement of additional ribs to the bond performance of FRP bars in concrete. Construction and Building Materials, 185, 545-554.

Li, Y., Yin, S., Lu, Y., & Hu, C. (2020). Experimental investigation of the mechanical properties of BFRP bars in coral concrete under high temperature and humidity. Construction and Building Materials, 259, 120591.

Ma, G., Huang, Y., Aslani, F., & Kim, T. (2021). Tensile and bonding behaviours of hybridized BFRP–steel bars as concrete reinforcement. Construction and Building Materials, 201, 62-71.

Maranan, G. B., Manalo, A. C., Karunasena, W., & Benmokrane, B. (2015). Pullout behaviour of GFRP bars with anchor head in geopolymer concrete. Composite Structures, 132, 1113-1121.

McVay, M., Cook, R. A., & Krishnamurthy, K. (n.d.). Pullout Simulation of Postinstalled Chemically Bonded Anchors. 122(9), 1016-1024.

Müsevitoğlu, A., Abdullah, M. H., Aksoylu, C., & Özkış, A. (2020). Ahmet. Measurement, 158, 107689.
Nilforoush, R., Nilsson, M., & Elfgren, L. (2017). Experimental evaluation of tensile behaviour of single cast-in-place anchor bolts in plain and steel fibre-reinforced normal- and high-strength concrete. Engineering Structures, 147, 195-206.

Obata, M., Inoue, M., & Goto, Y. (1998). The failure mechanism and the pull-out strength of a bond-type anchor near a free edge. Mechanics of Materials, 28(1-4), 113-122.

Pinoteau, N., Pimienta, P., Guillet, T., Rivillon, P., & Rémond, S. (2011). Effect of heating rate on bond failure of rebars into concrete using polymer adhesives to simulate exposure to fire. International Journal of Adhesion and Adhesives, 31(8), 851-861.

Porcarelli, S., Shedde, D., Wang, Z., Ingham, J. M., Giongo, I., & Dizhur, D. (2021). Tension and shear anchorage systems for limestone structures. Construction and Building Materials, 272, 121616.

Richardson, A. E., Dawson, S., Campbell, L., Moore, G., & Mc Kenzie, C. (2019). Temperature related pull-out performance of chemical anchor bolts in fibre concrete. Construction and Building Materials, 196, 478-484.

Rosa, I. C., Firmo, J. P., Correia, C. R., & Mazzuca, P. (2021). Influence of elevated temperatures on the bond behaviour of ribbed GFRP bars in concrete. Influence of elevated temperatures on the bond behaviour of ribbed GFRP bars in concrete, 122, 104119.

Shirvani, M., Klingner, R. E., & Graves III, H. L. (2004). Breakout Capacity of Anchors in Concrete Part 1: Tension. Structural Journal, 101(6), 812-820.
Stehle, E. J., & Sharma, A. (2021). Concrete cone breakout behavior of anchor groups in uncracked concrete under displacement-controlled cyclic tension load. Engineering Structures, 246, 113092.

Sun, W., & Ghannoum, V. M. (2015). Modeling of anchored CFRP strips bonded to concrete. Construction and Building Materials, 85, 144-156.
Takase, Y. (2019). Yuya. Engineering Structures, 195, 551-558.

Vita, N., Sharma, A., & Hofmann, J. (2022). Bonded anchors with post-installed supplementary reinforcement under tension loading – Experimental investigations. Bonded anchors with post-installed supplementary reinforcement under tension loading – Experimental investigations, 252, 113754.

Wang, Q., Zhu, H., Tong, Y., Su, W., & Zhang, P. (2021). Bond-slip behaviour of the CFRP ribbed bars anchored with the innovative additional ribs in concrete. Composite Structures, 262, 113595.

Yilmaz, S., Özen, M. A., & Yardim, Y. (2013). Tensile behavior of post-installed chemical anchors embedded to low strength concrete. Construction and Building Materials, 47, 861-866.

Zamora, N. A., Cook, R. A., Konz, R. C., & Consolazio, G. R. (2003). Behavior and Design of Single, Headed and Unheaded, Grouted Anchors under Tensile Load. Structural Journal, 100(2), 222-230.

Zhang, H., Smith, S. T., Gravina, R. J., & Wang, Z. (2017). Modelling of FRP-concrete bonded interfaces containing FRP anchors. Construction and Building Materials, 139, 394-402.